COSMIC SHEAR WITH ANTU/FORS1:
An Optimal Use of Service Mode Observation

R. MAOLI[1,2,3], Y. MELLIER[2,3], L. VAN WAERBEKE[2,4], P. SCHNEIDER[5,6], B. JAIN[7], T. ERBEN[6], F. BERNARDEAU[8], B. FORT[2], E. BERTIN[2,3], M. DANTEL-FORT[3]

[1]*Dipartimento di Fisica, Università di "Roma La Sapienza", Italy;* [2]*Institut d'Astrophysique de Paris, France;*
[3]*Observatoire de Paris, DEMIRM, France;* [4]*Canadian Institute for Theoretical Astrophysics, Toronto, Canada;*
[5]*Institut für Astrophysik und Extraterrestrische Forschung, Bonn, Germany;* [6]*Max-Planck-Institut für*
Astrophysik, Garching, Germany; [7]*Department of Physics, Johns Hopkins University, Baltimore, USA;*
[8]*Service de Physique Théorique, C.E. de Saclay, France.*

The measurement of weak gravitational lensing induced by large-scale structures is one of the most challenging programmes for imaging with ground-based telescopes. The VLT, used in Service Mode, offers an exceptional technical configuration which in principle guarantees high-quality data for demanding programmes. The first attempt done in Period 63 turned out to work very well and provides a remarkable data set on a short time-scale as well as first constraints on cosmological models. It demonstrates that the VLT is a perfectly suited telescope for cosmic shear measurements. Moreover, when it is operated in service mode, this is the most competitive ground-based tool which could make a major breakthrough in the field.

1. Introduction

At the beginning of 2000, four groups have announced the detection of a "cosmic shear" signal in deep field images. Among those works, one resulted of VLT observations we obtained on UT1/ANTU during its first year of operation. These results produced a strong excitement in the community who realised the fantastic interest of cosmic shear for cosmology.

Light beams emitted by distant galaxies can be altered by the gravitational field of groups, clusters or filaments of (dark) matter they cross during their propagation through the universe. The weak gravitational lensing effects accumulated along a line of sight result in a small distortion of the shape of background galaxies which can be observed on CCD images as a correlated ellipticity distribution of the lensed sources (the cosmic shear).

The properties of these gravitational lensing effects are characterised by an anisotropic deformation (a vector, the gravitational shear,) and an isotropic rescaling (a scalar, the gravitational convergence,). The convergence is directly related to the projected mass density accumulated along a line of sight. It turns out that in the weak lensing regimes, the shear and the convergence are linearly related.

The analysis of the cosmic shear signal as function of angular scales (between 10 arcseconds to about one degree) has an important scientific potential for cosmology (see Mellier 1999; Bartelmann and Schneider 2000 and references therein). The cartography of the distortion field traced by lensed galaxies can be used to reconstruct the projected mass density and the shape of the power spectrum of the dark matter, without regard to the light distribution. When these mass maps are cross-correlated with galaxy redshift surveys, one can also probe the evolution of the biasing as function of angular scale and its evolution with look-back time. Moreover, the normalisation of the power spectrum and the cosmological parameters can be inferred from the second and third moments of the gravitational convergence, $\kappa^2 (\theta)^{1/2}$ and $S_3 (\kappa)$, which are also sensitive to cosmological models (Bernardeau et al. 1997):

$$ 0.01 \ _8 \ ^{0.8} \left(\frac{}{1\text{deg.}} \right)^{-\frac{n+2}{2}} z_s^{0.75}, \quad (1)$$

and

$$ S_3 (\ ) \quad 40 \ ^{-0.8} z_s^{-1.35}, \quad (2)$$

where $_8$ is the normalisation of the power spectrum of density fluctuations, the density parameter and z_s the redshift of the lensed sources[1]. Therefore, by measuring these two quantities, one can recover and the normalisation of the power spectrum independently. Setting aside the technical difficulties,

the measurement of the second moment looks in particular an easy task because in the weak lensing regime the variance of the convergence is the variance of the gravitational shear. So, in principle it can be measured directly from the measurement of ellipticities of galaxies.

The expected amplitude of the gravitational distortion is extremely small (the ellipticity induced by weak lensing is only a few per cent) which makes the observations among the most challenging in optical astronomy. Because this programme needs high image quality, the HST seems well suited to study cosmic shear. However, its small field of view cannot realistically survey many fields of view as large as 10 arcminutes over a large fraction of the sky. In contrast, ground-based telescopes can easily observe wide fields and are indeed efficient tools to carry out this type of surveys, provided the data fulfil the following criteria:

• high image quality in order to accurately measure shapes of very faint galaxies,

• deep observations in order to get a high galaxy number density and to minimise Poisson noise on small angular scales,

• a large number of fields spread over a large fraction of the sky, in order to minimise the field-to-field fluctuations produced by cosmic variance,

• a homogeneous data set which permits to obtain the shape of about 100,000 galaxies observed in almost the same conditions and to measure statistical quantities from a homogeneous sample,

which require an optimised design of the observing strategy. Unfortunately, it turns out that classical observing modes of ground-based telescopes are inefficient in providing large amounts of data on a short time-scale. Experienced visitor observers are aware that weather conditions are never stable
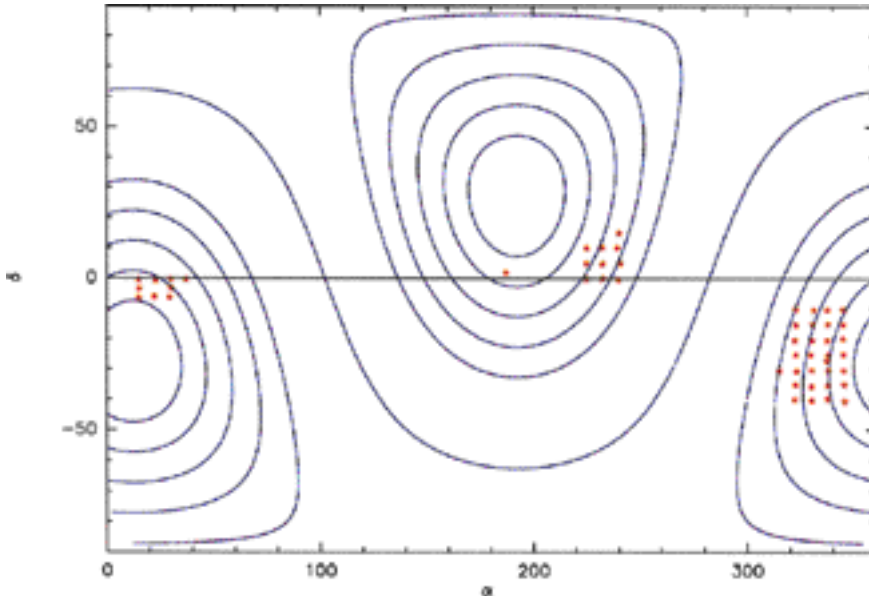
---

[1]This is the averaged redshift of the lensed sources. Since it is not necessary to get a precise measure of it, one can get a reasonable estimate from photometric redshift of galaxies.

Figure 1: Distribution on the sky of the 50 VLT fields. Continuous lines are for galactic latitudes b = 0, ±30, ±40, ±50, ±60, ±70. Contrary to the apparent distribution shown on this figure, the fields are not selected on a regular grid.

enough over a long period to succeed in a survey with demanding constraints. The best strategy is probably Service Mode, where observations are done by a staff of astronomers in charge of scheduling each night depending on the weather conditions and the recommendations of the OPC. When this mode is coupled with a very large telescope and an instrument with high image quality like FORS1, the constraints enumerated above are no longer critical. In fact, this configuration looks perfectly suited for a cosmic shear survey.

2. Selection and Observations of the Fields

In Period 63, we proposed to observe 0.6 deg^2 with FORS1 spread over 2000 deg^2 of the sky in order to measure the cosmic shear on many uncorrelated fields. Our scientific goals were[2] (1) the detection of cosmic shear on scales below 10 arcminutes, (2) the analysis of the variance of the gravitational shear as a function of angular scale and (3) the acquisition of a very large number of fields in order to minimise the noise contribution due to cosmic variance. We were granted 32 hours in Service Mode and Priority A (programme 63.O-0039A; PI: Mellier). Our specifications were the following:

• observation of a sample of 50 FORS1fields totalising an area of 0.6 deg^2, which is a minimum request in order to get a signal-to-noise ratio higher than 3 on the cosmic shear signal;

• a selection of fields, free of bright stars, over a large part of the sky in order to provide targets for any period during the semester. We pre-selected 120 fields with no bright star or bright/big galaxies. Note that "empty fields" is not a good selection criterion since it would bias the sample towards low-density regions instead of sampling the full mass range of structures in the universe;

• observation in I-band in order to keep the image quality as good as possible. Since we were informed that FORS1 has no fringes with the common broad band filter, I-band was the best choice for the programme. The I-band also offers the possibility to observe during grey or dark time;

• exposure time of 36 minutes per field, split in 6 × 6 minutes individual frames. Each was offset in order to remove bad pixels, cosmic rays, and to produce many different frames for the master flat field. The total exposure time was chosen in order to reach I = 24.5 (5, 3 arcseconds aperture) for the lensed galaxies. We then expected a galaxy number density of about 40 arcmin^{-2} per field and an effective redshift distribution with z ≈ 1;

• observations acceptable during non-photometric nights, since the photo-

metric stability is not critical for the measurement of cosmic shear;

• image quality with seeing lower than 0.8 arcsecond for all exposures.

From an observational point of view, the request for images acceptable during grey time and non-photometric nights, with targets covering the whole semester, eases the scheduling and the set-up of the instrument. The seeing specification is also reasonable when compared to the average seeing on Paranal. Paradoxically, although this programme looks very difficult to implement on ground-based telescopes in visitor mode, it can be easily scheduled and completed by astronomers in charge of service observations.

The preparation of the Observing Blocks (OBs) of 6 × 50 observations was also a new experience and a bit of concern since no one prepared such a large number of targets before. Fortunately, we had experienced most of the problems one year earlier, when we expected to make these observations in service mode with the NTT. For technical reasons this never happened but we had to prepare our targets with a very first version of the Phase II Proposal Preparation interface (P2PP) which forced us to interact with the User Support Group of the Data Division Management (DMD) in charge of P2PP. In order to work closely with the User Support Group, we prepared the files at ESO in Garching, which turned out to be the most efficient way to learn and to improve this interface for survey cases. All our requests and the problems we faced were immediately addressed and fixed very quickly by the DMD. When Period 63 started, the improvements done in P2PP made the preparations of the OBs an easy task. The final sample defined on the OBs is plotted in Figure 1.

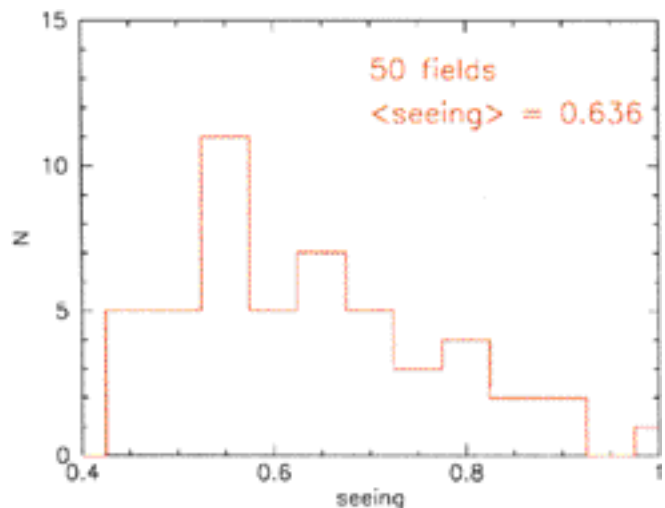Observations were done between May and September 1999 with FORS1. During the semester, we were continu-

Figure 2: Histogram of the seeing for the 50 final coadded fields.

11

ously informed on the status of the observations by monitoring the progress of the observations on the ESO web pages[3]. The comments made for each observation provide some details on the conditions with respect to our specifications, so we had a rather good idea of the success of the programme prior to proceed to thorough investigations at the TERAPIX data centre at the Institut d'Astrophysique de Paris (IAP). The programme was completed in due time by September 1999, and the CD-ROMs containing the data were received at IAP by the end of November 1999.

3. Analysis of VLT/FORS1 Data

Each image was overscan corrected, bias subtracted and flatfielded with a superflat computed with the exposures taken during the same night. The FORS1 images are read through four ports readout, so we processed separately the image subsets coming from the four quadrants of the CCD. Then we normalised the gain of each quadrant to obtain an image with a homogeneous background. Finally, we aligned the six individual exposures to produce the final stacked image. An example of one of the 50 FORS1 fields is given in Figure 3.

At this stage, the images are ready for weak lensing analysis. It consists in measuring the ellipticity of all galaxies, correcting their apparent shape for the atmospheric and optical distortions, and then recovering the lensing signature.

The corrections are done assuming that the smearing and the circularisation produced by the atmosphere and the instrument are small. Kaiser et al. (1995, hereafter KSB) have developed an efficient algorithm which expresses the linear corrections and permits to recover easily the lensing signal. If one defines the ellipticity of the source as function of the second moments of the image

$$\mathbf{e} = \left(\frac{I_{11} - I_{22}}{\mathrm{Tr}(I)}, \frac{2I_{12}}{\mathrm{Tr}(I)} \right) \text{ with}$$
$$I_{ij} = \int \mathrm{d}^2\beta \; W(\beta)\beta_i\beta_j \, f(\beta), \qquad (3)$$

then the observed ellipticity can be expressed by the KSB formalism,

$$\mathbf{e}^{\mathrm{obs}} = \mathbf{e}^{\mathrm{source}} + P_\gamma \gamma + P^{\mathrm{sm}}\mathbf{p} \qquad (4)$$

where $\mathbf{e}^{\mathrm{source}}$ is the intrinsic ellipticity of the source, P^{sm} *is the smear polaris - ability tensor* associated with the effects produced by the anisotropic part of the PSF, expressed by $\mathbf{p}$, and P is the *shear polarisability tensor* which expresses the effect of the response of
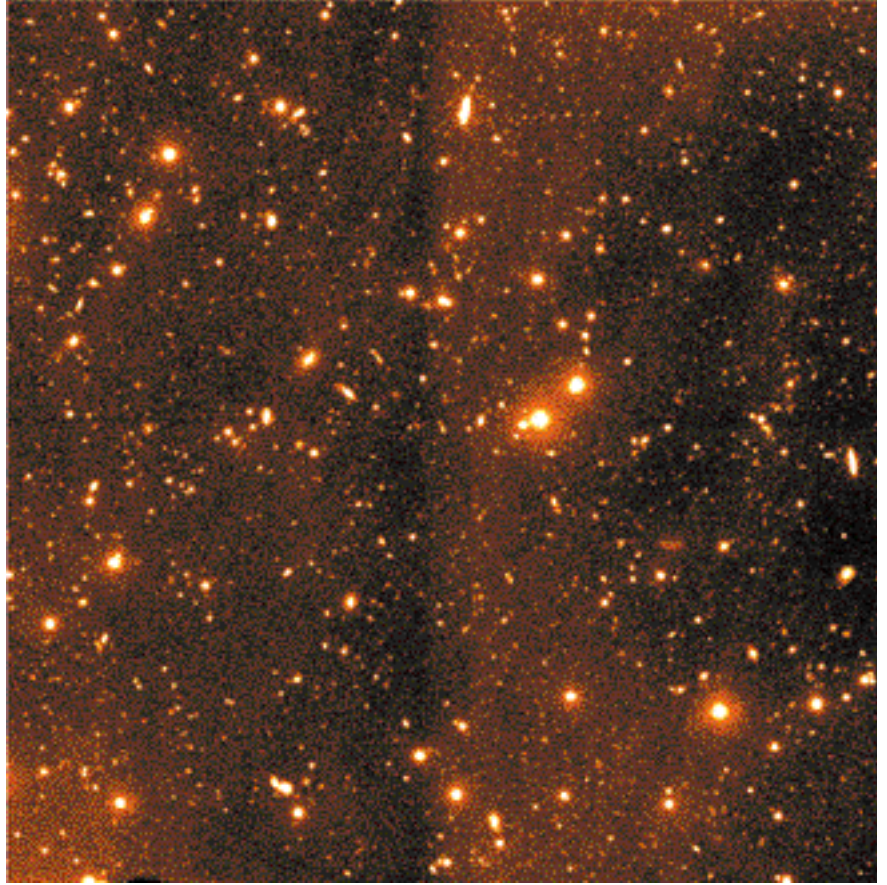
Figure 3: Final coadded image of a VLT field. In this case the FWHM of the stellar images is 0.53″, the source density is 35.3 galaxies/arcmin², with a 6.5′ × 6.5′ field and with 67 unsaturated stars.

a source to a gravitational shear. These tensors are complicated functions which depend on the profile of the light distribution. They can be calculated directly from the image profiles.

Both $\mathbf{p}$ and can be deduced from the data. The former is determined from the field stars, which are not gravitationally distorted and which must be circular objects once corrected for atmospheric and instrumental effects. On the other hand, if we assume that there is no preferred direction for the intrinsic ellipticity of the sources (i.e. the galaxies), then the averaged ellipticity of the sources is $\mathbf{e}^{\mathrm{source}} = 0$, and the mean shear at a given angular scale is

$$\gamma = \langle P^{-1}, \mathbf{e}^{\mathrm{obs}} - P^{\mathrm{sm}}\mathbf{p} \rangle \qquad (5)$$

where the average (and therefore its variance) is computed over the angular scale .

The selection of stars for PSF correction and the selection of galaxies for the measurement of the gravity-induced ellipticity are obtained by the following sequence (for details, see Figure 4 and van Waerbeke et al. 2000):

1. Masking: on each image, we remove the boundaries of the CCD as well as the central cross delineating the four quadrants. Areas around bright stars, bright galaxies and satellite traces are also removed;

2. Star selection: we use a radius[4] vs. magnitude diagram to select unsaturated stars (see Fig. 4). Note that the stars in a given image have all the same radius given by the seeing. Thus, in the diagram, they fall along a thin vertical line (indicated by a red arrow). In the example in Figure 4, their radius rh = 2 corresponds to a FWHM of 0.8 arcsec with a detector having a scale of 0.2 arcsec per pixel. The stars are selected along the central domain of the thin vertical branch of the diagram where there is no confusion with galaxies and no saturated stars;

3. Fit of the stellar polarisability tensors: using stars, we map the PSF by fitting their shape over the CCD with a third-order polynomial;

4. Shear estimate computation: using the stellar fits, we compute Eq. 5 for all the sources;

5. Source selection: finally, galaxies are selected using the star/galaxy classification defined in SExtractor (Bertin & Arnouts 1996). All objects with ambiguous classification and close pairs of galaxies are removed from the sample.
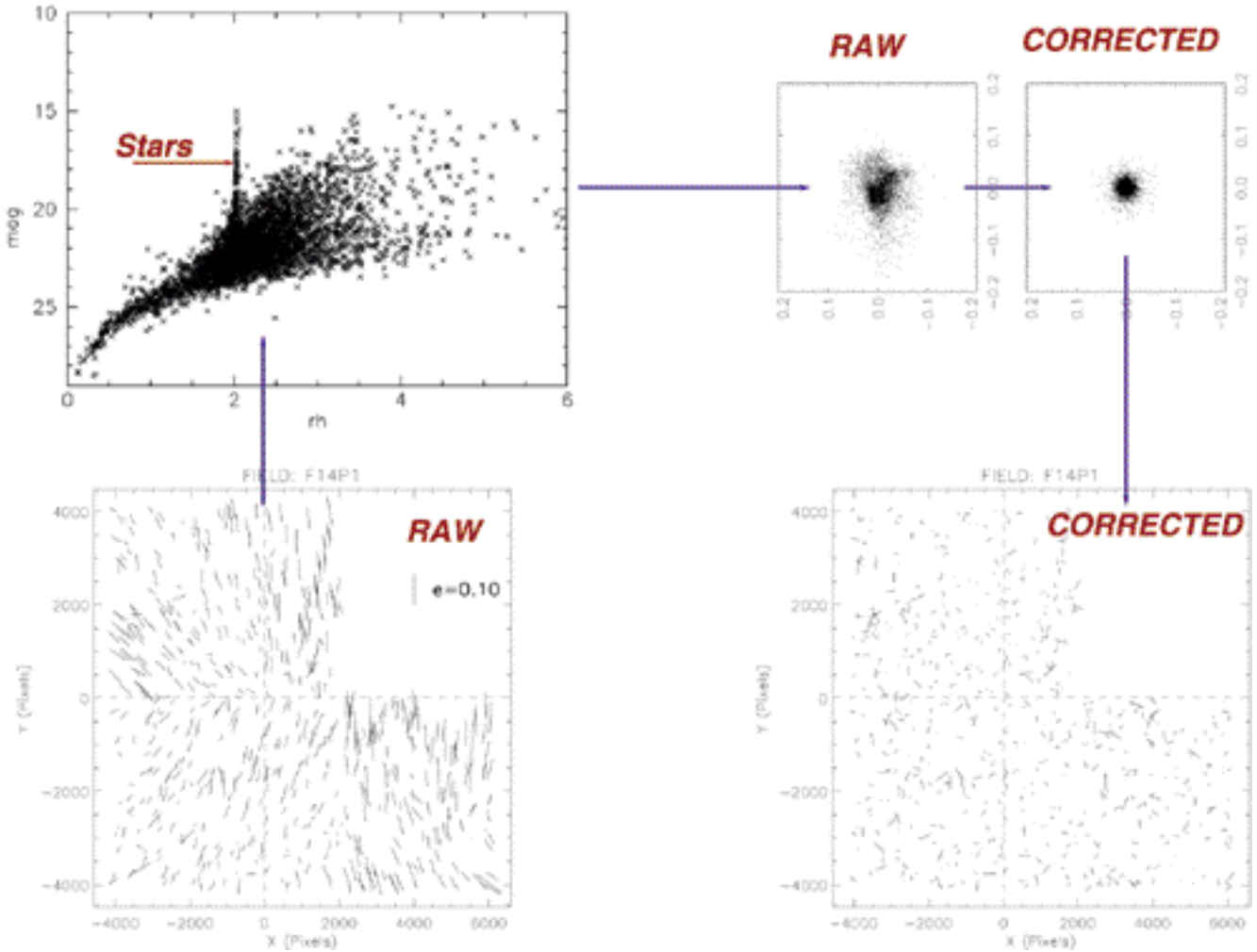
Figure 4: The PSF correction procedure using the stars selected from the rh vs. mag. diagram. The bottom-left panel shows the ellipticity of the stars before correction. The lines indicate the position, the elongation and the orientation of each object (this is an example, not a FORS1 field). The automatic identification of the stars is done using the rh vs. mag. diagram shown on the top-left panel. The stars can be easily identified from their location along the vertical line. Using the stars, the PSFcan be estimated anywhere in the CCD, from which one can re - cover the corrections to apply. The top-right panel shows the ellipticities of the uncorrected and corrected stars. We usually characterise the shape of objects in the $(e_1 = e \cos (2\beta), e_2 = e \sin (2\beta))$ plane, where e is the amplitude of the ellipticity and β the orientation with respect to the horizontal axis. If the correction is well determined, the final distribution should be isotropic with respect to the central position of the pan - el. The bottom-right panel shows the shape of the stars, once corrected, on the CCD.

In Figure 5 we plot the star elliptici-ties for all VLT fields before and after the PSF correction. The procedure works very well, except for a few cases which correspond to fields where the image quality is far from our specifica-tions (seeing significantly altered by strong wind). We ended up with 45 fields with in average 60 stars/field (a minimum of 20 and a maximum of 120) and a total number of 58,700 galaxies for 1900 arcmin^2, that is ~ 31 galaxies/arcmin^2 and 1300 galaxies/ field. It is worth noticing that 45 of 50 fields turn out to be very good for the cosmic-shear analysis, which means that the efficiency of the programme in service mode is 90% after 32 hours of service observing. For comparison, in visitor mode on a 4-metre telescope

and assuming 50% of good weather condition (clear night and seeing below 0.8), one would need about 25 nights...

4. Cosmology with Cosmic Shear

For each final corrected image, we computed the variance of the shear, ^{2} , using a top-hat window function with angular diameter varying from one to five arcminutes. Then we averaged ^{2} over the 45 fields. In this way we can associate an error to the value of ^{2} at a given angular scale . It is im-portant to stress that with 45 fields, we also have a fairly good estimate of the field-to-field fluctuation produced by the cosmic variance.

In Figure 6 we plot our results to-gether with the recent measurements of other cosmic shear surveys. Note the remarkable agreement between the results of the VLT and the results of other programmes conducted with dif-ferent observational strategies and dif-ferent instruments. This is a strong in-dication that the signal is of cosmolog-ical nature and not produced by sys-tematic effects.

Prediction from different cosmo-logical models are also plotted in the figure. The joint use of all the data sets puts very tight constraints on the shear amplitude on those scales, in particular with respect to theoret-ical expectations of the COBE-nor-malised standard CDM, which is ruled out at a 5- confidence level. This ex-

ample illustrates the potential of cosmic shear for cosmology. The data fit also most popular models, in particular in the range 2–10 arcminutes, where the averaged signal obtained by the various surveys provides a cosmic shear amplitude with very high signal-to-noise ratio. We are indeed very close to be able to constrain also these models.

The observations done with ANTU provide many more random fields than any other cosmic shear surveys done so far, which for the first time permits to beat the noise distribution generated by the cosmic variance. However, the errors are still too large to give precise estimates for the cosmological parameters and for the normalisation of the power spectrum of primordial density fluctuations. Only a larger amount of data will allow to reach this important goal. We have simulated the amount of data one would need in order to increase the signal-to-noise ratio by a factor of 3. It turns out that with 300 FORS1 fields obtained in service mode (that is 250 more fields than what we got, or 160 hours) we could separate the three other models plotted in Figure 6. This number of fields can be reduced to 150 if we use jointly the CFHT data and the other surveys going on at other telescopes.

On a longer time-scale, the observation of weak gravitational distortion of galaxies will be used to reconstruct the power spectrum of the dark matter up to 100 Megaparsec scales.
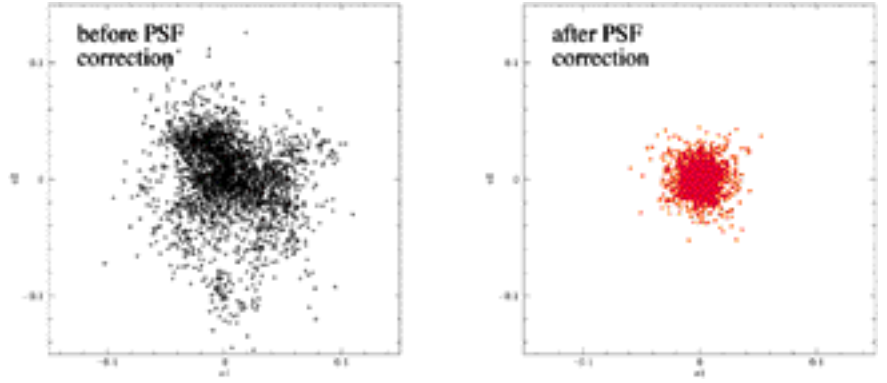

Figure 5: Star ellipticities before (at left) and after (at right) the PSFcorrection, for all the 45 selected VLT fields. A good PSFcorrection implies a zero mean value for e_1 and e_2 with small symmetric deviations.

This is a much more difficult project which in particular demands to map angular scales up to few degrees (Figure 6 shows that beyond 10 arcminutes there are discrepancies between the surveys, which express that the signal is very weak). This is beyond the reach of FORS1 which has a rather small field of view. But the WFI at the 2.2-m and maybe VIMOS on UT3, are excellent instruments for such a project. The image quality and performance of VIMOS for a weak lensing survey will be known this fall[5]. If the tests are positive, then this instrument could

easily cover degree-scale fields and provide superb data for cosmic shear, if the survey is carried out in service mode.

Acknowledgements

_____
[5]see http://www.astrsp-mrs.fr/virmos/vimos.htm for preliminary tests.

References

Bacon, D., Réfrégier, A., Ellis, R.S. *MNRAS,* submitted (2000).
Bartelmann, M., Schneider, P. *Phys. Rep.,* in press (2000).
Bernardeau, F., van Waerbeke, L., Mellier, Y., *Astr. & Astrophys.* **322**, 1 (1997).
Bertin, E., Arnouts, S., *Astr. & Astrophys.* **117**, 393 (1996).
Kaiser, N., Squires, G., Broadhurst, T., (KSB), 1995, *Astrophys. J.* **449**, 460.
Kaiser N., Wilson G. & Luppino G., 2000, *Astrophys. J. submitted,* astroph/ 0003338.
Maoli, R., Mellier, Y., van Waerbeke, L., Schneider, P., Jain, B., Erben, T., Bernardeau, F., Fort, B., 2000, astroph/ 0008179.
Mellier, Y., *Ann. Rev. Astr. & Astrophys.* **37**, 127 (1999).
van Waerbeke, L., Mellier, Y., Erben, T., *et al., Astr. & Astrophys.* **358**, 30 (2000).
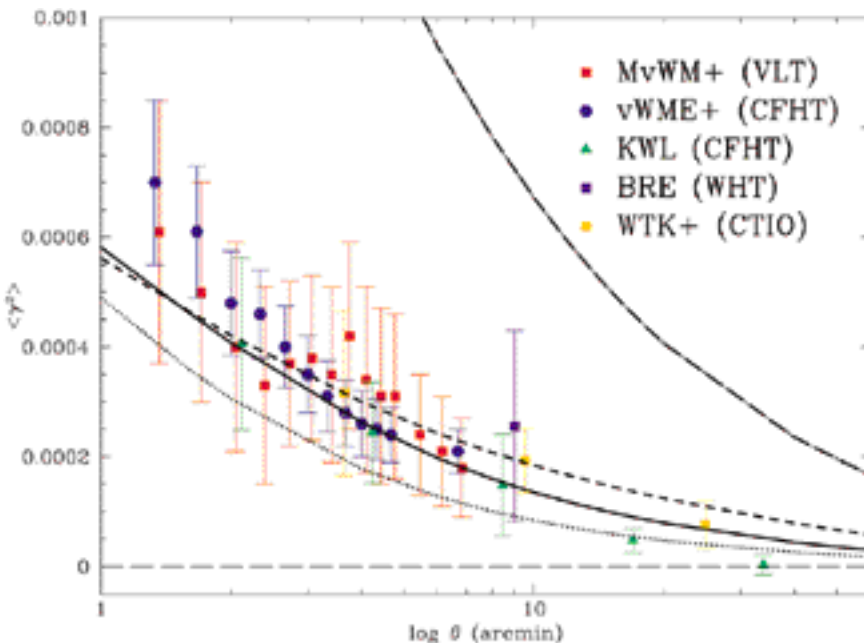Wittman, D.M., Tyson, A.J., Kirkman, D., Dell'Antonio, I., Bernstein, G. (2000), *Nature* **405**, 143.

Figure 6: Summary of cosmic shear measurements plotted as function of the angular scale θ. The work described here is referred to as MvWM+ (Maoli et al. in preparation; see Maoli et al. 2000), the other results are from van Waerbeke et al. 2000 (vWME+), Kaiser et al. 2000 (KWL), Bacon et al. 2000 (BRE) and Wittman et al. 2000 (WTK+). Some predictions of cosmological models are also plotted, assuming sources at $z_{eff} = 1$. The solid line corresponds to λCDM, with $\Omega_m = 0.3$, $\Omega_\Lambda = 0.7$, $\Gamma = 0.21$; the dot-dashed line corresponds to COBE-normalised SCDM; the dashed line corresponds to cluster-normalised SCDM and the dotted line corresponds to cluster-normalised Open CDM with $\Omega_m = 0.3$.